Forever young: how AHL15 delays developmental phase transitions to prevent ageing in plants

Luden, T.

Chapter 3

GreenLeafVI: An ImageJ plugin for high-throughput analysis of leaf chlorophyll content

Thalia Luden[1†], Jelmer van Lieshout[1†], Sarah Mehrem[3], Basten Snoek[3], Joost Willemse[2], Remko Offringa[1]

[1] Plant Developmental Genetics and [2] Cell Observatory, Institute of Biology Leiden, Leiden University, Sylviusweg 72, 2333 BE Leiden, The Netherlands

[3] Bioinformatics, Biodynamics and Biocomplexity, Utrecht University, Padualaan 8, 3584 CH Utrecht, The Netherlands

[†] These authors contributed equally to this work

Abstract

Leaf chlorophyll content is a strong predictor of plant health, and chlorophyll breakdown is a central process during leaf senescence. Chlorophyll quantification can be done in several ways, many of which are time-consuming or require specialized equipment. An alternative to this is the use of image-based chlorophyll estimation, which relies on the color values in RGB images that are used to calculate colorimetric visual indexes that indicate the leaf chlorophyll content. Image-based chlorophyll measurement is non-destructive and apart from a digital camera requires no specialized equipment. Here, we developed the ImageJ plugin GreenLeafVI that facilitates high-throughput image analysis for measuring leaf chlorophyll content. Our plugin offers the option to white-balance images to decrease variation between images, and has an optional background removal step. We show that this method can reliably quantify leaf chlorophyll content in a variety of plant species. In addition, we show that image-based chlorophyll quantification can replicate GWAS results based on traditional chlorophyll extraction methods, showing that this method is highly accurate.

Keywords: ImageJ, chlorophyll, leaf senescence, image-based chlorophyll quantification, high-throughput phenotyping

Introduction

Plant health can in many cases be deducted from the leaf chlorophyll (Chl) content, as several stressing factors can affect the photosynthetic capacity of plants. Chl content can be reduced by, for example, drought and salt stress, nutrient deficiency, pathogen infection, and other stressors (Hörtensteiner and Kräutler, 2011). Quantification of Chl is therefore an important tool to monitor plant health in a variety of conditions. Various methods for measuring Chl content can be applied, such as acetone-based Chl isolation followed by photospectrometry at 645 nm and 663 nm (Arnon, 1949), SPAD (Soil Plant Analysis Development) measurement (Yadava, 1986; Markwell et al., 1995; Konica Minolta Optics, 2009), Chl fluorescence measurement (Murchie and Lawson, 2013; Legendre et al., 2021), hyperspectral imaging (Zhang et al., 2022a; Taha et al., 2024), and image-based colorimetric visual index (CVI) estimations of Chl (Ali et al., 2012; Bresson et al., 2018; Guendouz et al., 2021). The acetone-based Chl extraction method directly measures the Chl content, and is one of the most accurate ways to quantify Chl. However, this method is labor-intensive and destructive, and requires specialized equipment to measure the OD_{645} and OD_{663}. Due to the destructive nature of this method, it is also poorly suited to monitor Chl content over a plant's development. Chl measurements with a SPAD meter are non-destructive, but SPAD measurements remain labor-intensive, as each measurement needs to be recorded manually, and SPAD values are strongly affected by the position on the leaf where the measurements are made. In addition, the SPAD meter can only be used on leaves above a certain size, which excludes the possibility to measure young or small leaves, or plants grown in tissue culture that need to remain in sterile conditions. Chl fluorescence measurements and hyperspectral imaging methods are non-destructive and can yield useful information, but require specialized equipment that can be expensive and are therefore not universally available to researchers. In addition, measuring Chl fluorescence makes use of the photo-saturation of Chl followed by a cool-down period, which makes this type of measurement relatively time-consuming. In contrast, image-based Chl quantification methods require only the use of a digital camera and uniform lighting, are non-destructive, and are highly adaptable to different environments and experimental setups. Because no specialized equipment is required, image-based Chl estimation can readily be applied in any environment and is almost universally available to all researchers. Moreover, digital images can be easily processed in batch, allowing high-throughput monitoring of Chl content in a variety of experimental setups (Prakash Yadav et al., 2010; Zhang et

al., 2018; Fernando Sánchez-Sastre et al., 2020; Guo et al., 2020; Özreçberoğlu and Kahramanoğlu, 2020; Guendouz et al., 2021; Zhang et al., 2022a; Taha et al., 2024).

Image-based Chl estimation relies on the relative pixel intensity in the Red, Green, and Blue channels of RGB images, from which Chl content can be deduced by using different mathematical models. Alternatively, values in the hue saturation value color-space (HSV) can be measured (Bresson et al., 2018). Various studies have shown the usefulness of RGB image analysis and their derived CVIs in estimating Chl content in different species, and strong correlations with total Chl content have been shown for many plant species. For example, Kawashima and Nakatani (1998) showed that the Chl content of wheat and rye leaves could be measured by using a video camera, and showed that the best predictor of Chl content was the normalized difference between the Red and Blue values (R-B)/(R+B), henceforth referred to as the Kawashima index. Other well-performing models that were tested by Kawashima and Nakatani include the normalized Red, Green, and Blue indexes (R/(R+G+B), G/(R+G+B), B/(R+G+B)), and the difference between red and blue divided by the sum of all channels ((R-B)/(R+G+B)). Ali et al. (2012) showed that the Kawashima index correlated strongly with SPAD-502 readings in tomato, and Taha et al. (2024) showed the same in hydroponically-grown lettuce. Similarly, Fernando Sánchez-Sastre et al. (2020) showed that the highest-scoring models tested by Kawashima and Nakatani (1998) also showed a strong correlation with Chl content in sugar beet leaves. On the other hand, Ibrahim et al. (2021) and Ali et al. (2012) found that the Green : Red ratio (G:R) correlated to Chl content in lettuce more strongly than the Kawashima index. Other researchers have used custom models to link the RGB color values to Chl content. For example, Prakash Yadav et al. (2010) showed that Chl content could be accurately measured in micro-propagated potato by using RGB images as well as by the hue, saturation, and intensity values derived from these images, and a similar approach was used in Sorghum by Zhang et al. (2022a). Other applications of the RGB color space have also been applied, for example by Govindasamy et al. (2017) who used RGB images to monitor the symbiosis efficiency between rhizobia and soybean plants, and Bu et al. (2024) who used RGB parameters to measure soybean pod freshness. Han et al. (2021) used aerial images to monitor the growth of *Hibiscus cannabinus* based on RGB-derived parameters, and Barraza-Moraga et al. (2022) applied RGB analysis to satellite images in order to estimate the Chl-A content of algae in lake Lanalhue in Chile. Overall, these examples show that analysis of RGB images can successfully be applied in plant research and

is a feasible method of Chl measurement.

The open-source software FIJI is a distribution of the image analysis program ImageJ, which is a commonly used and highly customizable tool for image analysis in the life sciences (Schindelin et al., 2012). FIJI offers possibilities to automate analysis steps via the use of macros or custom-made plugins. In order to enhance the throughput of RGB image analysis, we developed the FIJI plugin called Green Leaf Visual Index (GreenLeafVI) that can perform multiple steps of RGB analysis in batch mode for a large number of images. GreenLeafVI offers the option to normalize image brightness, segment images to reduce background noise, and calculate the RGB values of multiple objects per image along with various methods of leaf Chl content estimation for a large number of images, allowing for high-throughput analysis. The output data is stored in a tidyR-compatible format that can readily be used for further statistical analysis in R or other statistics software. We show that GreenLeafVI can be applied for measuring Chl content of different plant species, and can accurately reproduce GWAS results obtained by traditional Chl measurement methods in lettuce, validating its use for high-throughput phenotyping experiments.

Methods

Plant materials and growth conditions

Arabidopsis thaliana (Arabidopsis) ecotype Col-0 seeds were sown on humid soil (90% turf, 10 % sand) and stratified at 4 °C for three days, and subsequently transferred to a growth chamber with long day conditions (16h light / 8h dark) at 21 °C and 65 % relative humidity. Seedlings were repotted to individual pots after 7 days, and the fifth leaf of each plant was harvested at 23 days after the end of stratification. Leaves incubated for 0-5 days in the dark were used for senescence measurements to represent various stages of leaf senescence.

For testing the correlation between colorimetric measurements and chlorophyll content, *Lactuca sativa* (lettuce) cv. Cobham green seeds were sterilized in 50% bleach solution and stratified in distilled water for 4 days at 4 °C. Subsequently, seeds were sown on moist soil (90% turf, 10 % sand) and transferred to a growth chamber with long day conditions (16h light / 8h dark) at 21 °C and 70 % relative humidity. The fourth leaf was harvested ten days after emergence, and 30 mm Ø leaf disks were taken and incubated on demineralized water with 1% agarose in the dark for up to 5 days. Leaves subjected to different dark incubation periods were used for senescence measurements to represent a range of senescence stages. For the GWAS experiment, lettuce seeds of 184

cultivars were treated as described above, and leaf disks of the fourth leaf were taken at 10 days after emergence and used directly for imaging and chlorophyll extraction.

Nicotiana benthamiana (tobacco) seeds were sown on moist soil (90% turf, 10 % sand) in a growth chamber with long day conditions (16h light / 8h dark) at 21 °C and 70 % relative humidity. After seven days, seedlings were repotted to individual pots. After three weeks, mature leaves were detached and incubated in large petri dishes on demineralized water with 1% agarose in the dark for up to seven days.

Solanum lycopersicum (tomato) cv. Moneymaker seeds were sterilized in bleach and germinated on solid MS medium, and transferred to soil after three weeks. Plants were grown in long days conditions (16h light/8h dark) at a 24 °C day / 18 °C night temperature regime. Leaves were harvested from flowering plants and incubated in large petri dishes on demineralized water with 1% agarose in the dark for up to seven days, with harvesting points between 0-7 days of dark incubation.

Senescence induction, imaging, and chlorophyll isolation

Arabidopsis leaves were floated on 5 mM MES buffer (pH 5.6) in 5 cm petri dishes sealed with parafilm, wrapped in aluminium foil, and kept at 21 °C for up to five days. Lettuce, tomato, and tobacco leaves were harvested at various ages and placed in petri dishes with demineralized water with 0.5% agarose, sealed with parafilm, wrapped in aluminium foil, and stored at 21 °C for up to 7 days. Leaves were imaged at different time points between 0 and 7 days of dark incubation and leaf disks were collected for chlorophyll extraction after imaging. All images were taken with a Nikon DC3000 DSLR camera under uniform white light. Plant leaves were placed on a homogenous white or black background along with a white square that served as a reference for image brightness.

Chlorophyll extraction was performed according to the protocol of Arnon et al. (1949). Briefly, 5 mm diameter round leaf disks were taken after imaging (2 for Arabidopsis, 3 for other species) and placed in a 96-well deepwell plate along with a metal bead and stored at -80 °C until extraction. For extraction, the leaf tissue was pulverized and resuspended in 200 µL 25 mM sodium phosphate buffer (pH 7) and 800 µL 80% (v/v) acetone. Samples were then incubated at room temperature in the dark for 1 hour with gentle shaking and centrifuged for 10 minutes at 3000 *g*. 200 µL of the supernatant was then transferred to a 96-well transparent-bottom plate and the absorption (D) at 645nm and 663

nm was measured with a TECAN reader. The total chlorophyll content in mg/L was then calculated with the following formula: $Chl_{Total} = 20{,}2 \cdot D_{645} + 8{,}02 \cdot D_{663}$ as described by Arnon (1949), and the amount of Chl in one mL (the extraction volume for each sample) was divided over the total area of leaf tissue used for extraction.

Image analysis

All images were analyzed using the FIJI distribution of ImageJ (Schindelin et al., 2012), with the custom GreenLeafVI plugin that can perform white balancing, automatic selection of leaves and removal of background, and RGB pixel intensity measurements semi-automatically. The plugin is described in detail in Supplementary protocol 1, and Figure 1 shows a schematic overview of the steps performed by the plugin.

White balancing

In order to calibrate the image brightness and reduce inter-image variation, we normalized the pixel intensity to the white reference area included in each image (Figure 1). This was done by splitting the image into Red, Green, and Blue channels and automatic measurement of the mean pixel intensity in the white reference area. Next, the pixel adjustment factor for each of the channels was calculated by dividing the maximum brightness (255 for 8-bit images) by the mean pixel intensity of the white area (adjustment factor = 255/mean). The white reference was then set to an intensity of 255 in all three channels, and the pixels outside of the reference area were normalized based on the adjustment factor for each channel, and re-stacked into an RGB image with a "_whitebalanced" suffix for further analysis.

Segmentation of images to reduce background

In order to exclude measurements of non-leaf objects or areas in the background of the image, we included an optional segmentation step in the GreenLeafVI plugin (Figure 1). The segmentation step extracts leaf-like objects from the background by creating a mask covering the leaves based on HSV and minimum area parameters, and removes the background by setting the pixel intensity outside of masked areas to 0. The HSV values used to distinguish leaves from the background were calibrated manually for each species. The images were then saved extended by a "_segmented" suffix for further analysis.

RGB analysis and color-based methods of chlorophyll estimation

To measure the R, G, and B pixel intensities of individual objects in an image, a mask selecting individual objects was made like in the segmentation step. The original image was then split into Red, Green, and Blue channels and the minimum, maximum, median, and mean pixel intensity was measured in each object of the mask covering the leaves (Figure 1). The mean values of each leaf measured in the Red, Green, and Blue channels were used to calculate the different visual indexes: Green:Red ratio (GR_ratio), Red:Green ratio (RG_ratio), Kawashima index (Kawashima), Green Leaf Index (GLI), Normalized Difference Index (NDI), normalized Red (Red_norm), normalized Green (Green_norm), normalized Blue (Blue_norm), and the Woebbecke index (Woebbecke).

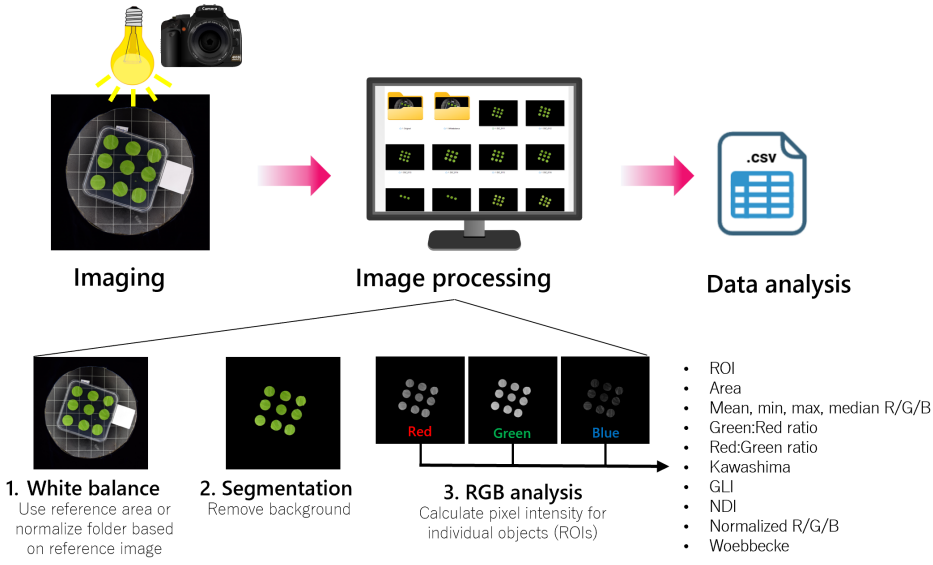

Figure 1: Workflow for high-throughput chlorophyll measurement with GreenLeafVI. Images are taken under homogeneous light with a white reference area. The images are then batch-processed for **1**) white-balancing based on the white reference area; **2)** segmentation to remove the background; and **3)** measurement of pixel intensity in the Red, Green, and Blue channels. The results of the RGB analysis are stored in a results.csv file which, in addition to the RGB values, also contains the region of interest (ROI) ROI, the area of the objects, and several colorimetric visual indeces (CVIs).

Data analysis

Correlation analyses

Data generated by the ImageJ plugin and from spectrophotometry results were analyzed in R (R Core Team, 2023). Pearson's correlation analysis between

the different colorimetric indexes and the total Chl content as mg Chl / cm^2 was performed with the R package psych (William Revelle, 2023), and plots were generated by using the ggplot2 (Wickham, 2016) and ggpubr packages (Kassambara, 2023).

GWAS analysis

SNP data was obtained from Dijkhuizen et al. (2024). Kinship was computed as the covariance matrix of SNPs using the cov() function in R. SNPs were filtered for a MAF > 0.05. For GWAS, we used R version 4.2.2 and the lme4QTL package (Ziyatdinov et al., 2018). GWAS was performed on the filtered SNP set using a linear mixed model (relmatLmer and matlm), with the kinship matrix included as a random effect. The Bonferroni method was used to correct for multiple testing, with the Bonferroni-corrected significance threshold being -log10(0.05/2,485,803) > 7.69. Manhattan plots were created using ggplot (Wickham, 2016). Quantile-Quantile (Q-Q) plots were created using the ggfastman R-package (Tremmel, 2021). The genome annotation and gene function prediction of the Salinas reference genome V8 were used for annotation of significantly associated loci (Reyes-Chin-Wo et al., 2017).

Results and discussion

Normalized Red and Green:Red ratio are accurate predictors of chlorophyll content in leaves

We designed the Green Leaf Visual Index (GreenLeafVI) plugin as a tool to easily phenotype the Chl content in different plant species. We therefore ran the three steps of the GreenLeafVI plugin (white balancing, segmentation, and RGB analysis) on four different plant species: *Arabidopsis thaliana* (Arabidopsis), *Nicotiana benthamiana* (tobacco), *Solanum lycopersicum* (tomato), and *Lactuca sativa* (lettuce). In addition, we extracted chlorophyll from each imaged leaf by a classical method in order to test how well the different CVIs measured by the GreenLeafVI plugin correlated to the actual Chl content. Our data show that several CVIs show a strong correlation with the total Chl content for these different plant species. Figures 2A-D show the correlation between the total Chl content in $mg \cdot cm^{-2}$ and the best scoring CVI for each of the four species (Pearson's correlation). Our results show that the CVI-based prediction of Chl is most accurate for lettuce, and that the Green : Red ratio (G:R) and Normalized Difference Index (NDI) are the most robust Chl predictors for this species (Figure 2D, Table 1). For Arabidopsis, tobacco, and tomato the normalized Red

value (Rn; R/(R+G+B)) best predicted Chl content, although the G:R and NDI correlated significantly with the Chl content as well (Figure 2A-C, Table 1).

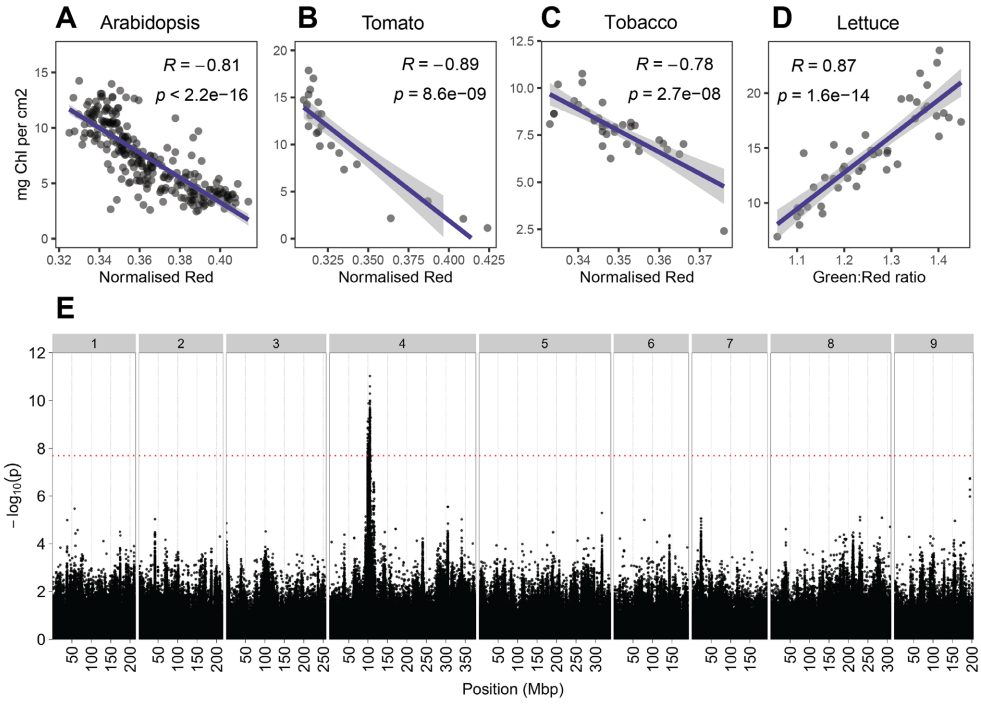

Figure 2: Application of CVIs for measuring chlorophyll content in different species. **A-D**: correlations between total Chl content as mg Chl/cm2 and the best-scoring CVI for each species. **A**: Arabidopsis, **B**: tomato and **C**: tobacco each show the strongest correlation between mg Chl·cm^{-2} and the normalized Red value (Rn). **D**: In lettuce, mg Chl·cm^{-2} correlates best with the Green : Red ratio (G:R). **E**: Manhattan plot of the GWAS on the Green : Red ratio measured on the fourth leaf of 184 lettuce cultivars. Genomic position, indicated in mega base pairs, is shown on the x-axis, chromosome numbers are indicated on top. Significance as – log10(p) is shown on the y-axis. The Bonferroni threshold of -log10(p) > 7.69 is indicated by the red horizontal line.

Table 1: Correlations of various CVIs with the chlorophyll content in mg Chl/cm2 (Pearson's correlation). In the formula column, R, G, and B stand for average Red, Green, and Blue pixel intensity values.

		Arabidopsis		Tomato		Tobacco		Lettuce	
Index	***Formula***	***R***	***p value***	***R***	***p value***	***R***	***p value***	***R***	***p value***
Green:Red ratio	G/R	0.73	7.35E-46	0.87	4.55E-08	0.62	6.09E-05	**0.87**	**1.61E-14**
Kawashima Index	(R-B)/(R+B)	-0.42	9.63E-13	-0.76	2.00E-05	-0.05	0.7600	0.46	0.0016
Normalized Red (Rn)	R/(R+G+B)	**-0.79**	**6.16E-60**	**-0.89**	**8.62E-09**	**-0.78**	**2.72E-08**	-0.82	5.92E-12
Normalized Green (Gn)	G/(R+G+B)	0.49	2.08E-17	0.71	0.0001	0.48	0.0034	0.81	3.11E-11
Normalized Difference Index (NDI)	(Rn-Gn)/(Rn+Gn+0.01)	-0.72	2.09E-45	-0.87	4.45E-08	-0.62	4.98E-05	**-0.87**	**1.37E-14**
Green Leaf Index (GLI)	(2G-R-B)/(2G+R+B)	0.48	2.43E-17	0.71	9.10E-05	0.47	0.0034	0.81	2.60E-11
Woebbecke Index	(G-B)/(R-G)	-0.11	0.0794	0.24	0.2667	0.74	2.50E-07	0.78	6.00E-10

Surprisingly, the correlation between the Chl content and the Kawashima index was not as strong as in earlier reports, and was outperformed by G:R, NDI, and Rn in all four species. This could be because the pixel intensity in the green channel is not used to calculate the Kawashima Index, despite the fact that Chl appears green in colour. Each of the best-performing indexes included green pixel intensity in their formulas. However, greenness alone is not sufficient to accurately predict Chl content, as the normalized Green value (Gn; G/(R+G+B)) showed only a moderate correlation with the Chl content. In addition, the Woebbecke Index correlated very poorly with the total Chl content per cm^2. This is because the Woebbecke Index formula does not handle yellow colours well, resulting in extremely negative values for yellowing leaves due to high R and low G values. Although the Woebbecke Index might be suitable to compare greenness among healthy, non-senescent plants, it is unsuitable for quantifying Chl in senescent leaves and using other, more consistent indexes such as Rn or G:R is advisable. Because we used leaves at various stages of senescence (non-senescent up to completely senesced) in our experiments, our data are representative for an array of conditions. Previous research may have focused on measurement of Chl content in healthy, young plants only, and have omitted using senescent or otherwise yellow leaves in the calibration of the index, which could explain why some indexes perform less well than in previous studies. In conclusion, our data shows that several visual indexes perform well in predicting Chl content, and that the Rn, G:R, and NDI indexes are all reliable, with the most reliable one depending on the species.

In order to test whether visual indexes are sufficiently accurate to identify phenotypic differences between genotypes, we ran a Genome-Wide Association Study (GWAS) on leaf Chl content in lettuce and applied the plugin in a high-throughput manner to analyse 446 images at once. We then compared our method to a previous study that used chlorophyll extraction to identify loci controlling leaf Chl content in lettuce (Zhang et al., 2022b). We used a panel of 184 lettuce genotypes and imaged the fourth leaf at 10 days after emergence. We then used an extensive SNP dataset to run a GWAS on G:R (the best-performing CVI for lettuce) as a measure of Chl content. From this GWAS, a significant peak on chromosome 4 was identified (figure 2E), which corresponded to the peak found by Zhang et al. (2022b) in their GWAS on extracted Chl data. This peak is associated with the lettuce *Golden-Like (LsGLK)* gene, which is an important regulator of chloroplast development. The similarity in outcomes between the two GWASs shows that our G:R data can reproduce the association between the Chl content phenotype and the

SNP located near the *LsGLK* gene, indicating that G:R is not only an accurate measure of Chl content, but is also a reliable method to identify a phenotypic vs genotypic association. In addition, digital images can be re-examined at a later time and may provide additional information next to Chl content, whereas this information is lost when using destructive methods of Chl quantification. Since making digital images and automated image processing is less labor-intensive and less costly than large-scale Chl extraction, we propose that this method be used in future applications.

Author contributions

TL, JvL, and RO designed the experiments. TL and JvL performed Chl extraction experiments, and JvL performed lettuce phenotyping for GWAS. Correlation analyses were done by TL, and SLM and BS performed GWAS analysis. JvL, TL, and JW wrote the ImageJ scripts. TL wrote the manuscript with input from all other authors.

Acknowledgements

We thank Jan Vink, Ward de Winter and Mariel Lavrijsen for technical support and Marion Larue, Karin Verkerk, and Kim Roos for help with phenotyping. This work was supported the graduate school green top sectors grant (grant nr. GSGT.2019.024) from the Dutch Research Council (NWO) to TL.

Literature

Ali M.M., Al-Ani A., Eamus D., Tan D.K.Y. (2012). A new image processing based technique to determine chlorophyll in plants. J Agric & Environ Sci **12**: 1323–1328.

Arnon D.I. (1949). Copper enzymes in isolated chloroplasts. Polyphenoloxidase in *Beta Vulgaris*. Plant Physiol **24**: 1–15.

Barraza-Moraga F., Alcayaga H., Pizarro A., Félez-Bernal J., Urrutia R. (2022). Estimation of chlorophyll-a concentrations in Lanalhue lake using Sentinel-2 MSI satellite images. Remote Sens **14**: 5647.

Bresson J., Bieker S., Riester L., Doll J., Zentgraf U. (2018). A guideline for leaf senescence analyses: from quantification to physiological and molecular investigations. J Exp Bot **69**: 769–786.

Bu Y., Hu J., Chen C., Bai S., Chen Z., Hu T., Zhang G., Liu N., Cai C., Li Y., et al (2024). ResNet incorporating the fusion data of RGB & hyperspectral images improves classification accuracy of vegetable soybean freshness. Sci Rep **14**: 1–13.

Dijkhuizen R.F., Eijnatten A.L. van, Mehrem S.L., Bergh E.S. van den, Lieshout J. van, Spaninks K., Kaandorp S., Offringa R., Proveniers M., Ackerveken G. van den, et al (2024). From aerial drone to QTL: Leveraging next-generation phenotyping to reveal the genetics of color and height in field-grown *Lactuca sativa*. bioRxiv 2024.11.07.622452.

Fernando Sánchez-Sastre L., S Alte da Veiga N.M., Miguel Ruiz-Potosme N., Carrión-Prieto P., Luis Marcos-Robles J., Manuel Navas-Gracia L., Martín-Ramos P. (2020). Assessment of RGB vegetation indices to estimate chlorophyll content in sugar beet leaves in the final cultivation stage. AgriEngineering **2**: 128–149.

Govindasamy V., George P., Aher L., Ramesh S. V., Thangasamy A., Anandan S., Kumar Raina S., Kumar M., Rane J., Annapurna K., et al (2017). Comparative conventional and phenomics approaches to assess symbiotic effectiveness of *Bradyrhizobia* strains in soybean (Glycine max L. Merrill) to drought. Sci Rep. doi: 10.1038/s41598-017-06441-3

Guendouz A., Bendada H., Benniou R. (2021). A comparative study of chlorophyll content estimation in barley (*Hordeum vulgare L.*) genotypes based on RGB (Red, Green, Blue) image analysis. Agric Sci Digest **42**: 68–71.

Guo Y., Yin G., Sun H., Wang H., Chen S., Senthilnath J., Wang J., Fu Y. (2020). Scaling effects on chlorophyll content estimations with RGB camera mounted on a UAV platform using machine-learning methods. Sensors **20**: 5130.

Han G.D., Jang G.J., Kim J., Kim D.W., Rodrogues R., Kim S.H., Kim H.J., Chung Y.S. (2021). RGB images-based vegetative index for phenotyping kenaf (*Hibiscus cannabinus L.*). PLoS One **16**: e0256978.

Hörtensteiner S., Kräutler B. (2011). Chlorophyll breakdown in higher plants. BBA **1807**: 977–988.

Ibrahim N.U.A., Aziz A., Jamaludin S., Harith D. (2021). Development of smartphone-based imaging techniques for the estimation of chlorophyll content in lettuce leaves. Food Res **5**: 33–38.

Kassambara A. (2023). ggpubr: "ggplot2" Based Publication Ready Plots.

Kawashima S., Nakatani M. (1998). An algorithm for estimating chlorophyll content in leaves using a video camera. Ann Bot **81**: 49–54.

Konica Minolta Optics I. (2009). A lightweight handheld meter for measuring the chlorophyll content of leaves without causing damage to plants. SPAD-502Plus.

Legendre R., Basinger N.T., van Iersel M.W. (2021). Low-cost chlorophyll fluorescence imaging for stress detection. Sensors **21**: 1–17.

Markwell J., Osterman J.C., Mitchell J.L. (1995). Calibration of the Minolta SPAD-502 leaf chlorophyll meter. Photosynth Res **46**: 467–472.

Murchie E.H., Lawson T. (2013). Chlorophyll fluorescence analysis: a guide to good practice and understanding some new applications. J Exp Bot **64**: 3983–3998.

Özreçberoglu N., Kahramanoglu I. (2020). Mathematical models for the estimation of leaf chlorophyll content based on RGB colours of contact imaging with smartphones: A pomegranate example. Folia Hortic **32**: 57–67.

Prakash Yadav S., Ibaraki Y., Dutta Gupta S. (2010). Estimation of the chlorophyll content of micropropagated potato plants using RGB based image analysis. Plant Cell Tiss Organ Cult **100**: 183–188.

R Core Team (2023). R: A Language and Environment for Statistical Computing.

Reyes-Chin-Wo S., Wang Z., Yang X., Kozik A., Arikit S., Song C., Xia L., Froenicke L., Lavelle D.O., Truco M.J., et al (2017). Genome assembly with in vitro proximity ligation data and whole-genome triplication in lettuce. Nature Communications 2017 8:1 **8**: 1–11.

Schindelin J., Arganda-Carreras I., Frise E., Kaynig V., Longair M., Pietzsch T., Preibisch S., Rueden C., Saalfeld S., Schmid B., et al (2012). Fiji: an open-source platform for biological-image analysis. Nat Meth **9**: 676–682.

Taha M.F., Mao H., Wang Y., ElManawy A.I., Elmasry G., Wu L., Memon M.S., Niu Z., Huang T., Qiu Z. (2024). High-Throughput analysis of leaf chlorophyll content in aquaponically grown lettuce using hyperspectral reflectance and RGB images. Plants **13**: 392.

Tremmel R. (2021). ggfastman 1.2.0. https://github.com/roman-tremmel/ggfastman,

Wickham H. (2016). ggplot2: Elegant Graphics for Data Analysis.

William Revelle (2023). psych: Procedures for Psychological, Psychometric, and Personality Research. https://cran.r-project.org/package=psych

Yadava U.L. (1986). A Rapid and Nondestructive Method to Determine Chlorophyll in Intact Leaves. HortScience **21**: 1449–1450.

Zhang H., Ge Y., Xie X., Atefi A., Wijewardane N.K., Thapa S. (2022a). High

throughput analysis of leaf chlorophyll content in sorghum using RGB, hyperspectral, and fluorescence imaging and sensor fusion. Plant Methods **18**: 1–17.

Zhang J., Li M., Sun Z., Liu H., Sun H., Yang W. (2018). Chlorophyll content detection of field maize using RGB-NIR camera. IFAC PapersOnLine **51**: 700–705.

Zhang L., Qian J., Han Y., Jia Y., Kuang H., Chen J. (2022b). Alternative splicing triggered by the insertion of a *CACTA* transposon attenuates *LsGLK* and leads to the development of pale-green leaves in lettuce. Plant J **109**: 182–195.

Ziyatdinov A., Vázquez-Santiago M., Brunel H., Martinez-Perez A., Aschard H., Soria J.M. (2018). lme4qtl: Linear mixed models with flexible covariance structure for genetic studies of related individuals. BMC Bioinformatics **19**: 1–5.

Supplementary Figures

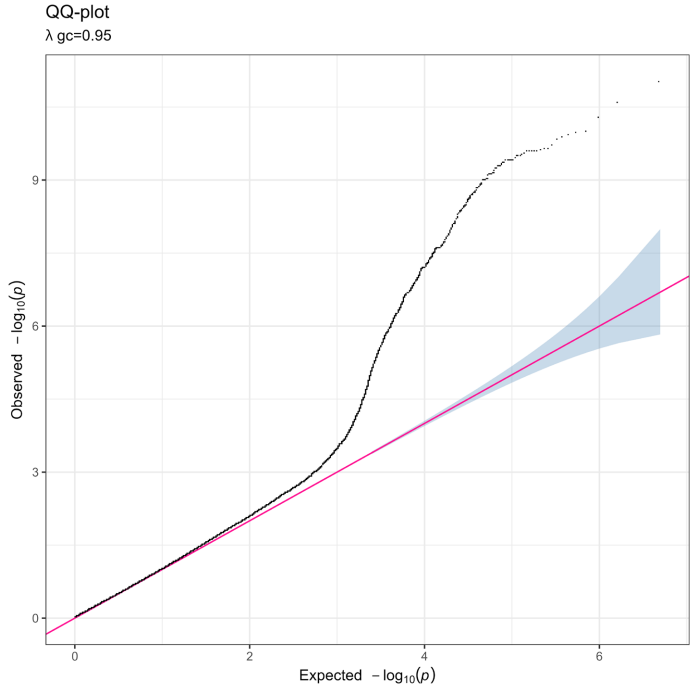

Supplementary figure 1: Quantile-Quantile plot for Green : Red ratio on the fourth leaf of 184 lettuce cultivars.

Supplementary protocol

Imaging setup and white balancing

The main limitation to image-based measurement is the variation in brightness and contrast between images. In order to calibrate the image brightness to reduce inter-image variation, we included an optional white-balancing step in the GreenLeafVI plugin (figure 1). The white-balancing step requires that a white reference area be photographed under the same conditions as the images to be analysed. This ensures that all images are white balanced to the same reference, reducing the variation in brightness between images that can arise from differential lighting or exposure settings during the imaging process. For this purpose, we recommend including a small white reference square or circle of a known size (e.g. 4 cm^2) in each of the images. This will serve as a reference for both the white balancing and for setting the image scale (via Analyze > set scale), which is useful for measuring the leaf area in addition to its Chl content. Alternatively, a single white reference area could be photographed at the start or end of the series of images to calibrate the entire set, assuming that lighting and exposure conditions are constant throughout the process.

When running the white balancing step, the user can select an input- and output folder and can select whether the images should be calibrated individually or batch-calibrated based on a single white reference image. Individual white balancing requires the user to select the reference area in each of the images and is therefore more time-consuming than the batch calibration, but is also more accurate and suitable for comparing images where the lighting, exposure, and focal distances are not constant. After the user has chosen whether to process images individually or in batch, the image is split into Red, Green, and Blue channels and the mean pixel intensity in the each channel is automatically calculated in the selected white area. Next, the pixel adjustment factor for each of the channels is calculated by dividing the maximum brightness of 8-bit images (255) by the mean pixel intensity of the white area (adj_factor = 255/mean). The white reference is then set to an intensity of 255 in all three channels, and the pixels outside of the reference area are then normalized based on the adjustment factor. Finally, the image is re-stacked to an 8-bit RGB image and saved in a folder selected by the user, and the image is saved under its original name with addition of a "_whitebalanced" suffix.

For optimal reproducibility between images, we recommend imaging under

constant lighting with a uniform background that shows sufficient contrast to the leaves that will be imaged such as a black, white, light blue, or orange background. In addition, variation between images can be further reduced by using the same focal distance between the camera and the leaves or plants that will be imaged throughout the process. If multiple objects are to be measured in one image, it is important that these do not overlap if a separate measurement of each object is desired.

Segmentation of images to reduce background

In order to exclude measurements of non-leaf objects or areas in the background of the image, we included an optional segmentation step in the GreenLeafVI plugin (figure 1). This process uses the difference in colour between the leaves and the background to extract only leaf-like objects. Because of this, the segmentation performs better when a background with an even colour that has sufficient contrast to the leaves is used during imaging, such as black, white, light blue, or orange. In order to run the segmentation process, the user needs to select an input- and output folder, and can adjust the settings for minimum object area, as well as minimum- and maximum values in the hue saturation value colour space (HSV). While the settings included in our plugin should perform well for any leaf-like object, we recommend that users customize these settings to the object of their interest to optimise segmentation performance. When the segmentation step is performed, a mask is created based on the HSV and minimum area inputs, and used to remove the background which is set to 0. The images are then saved in a folder selected by the user under their original name extended by a "_segmented" suffix.

RGB analysis and colour-based methods of chlorophyll estimation

The main feature of the GreenLeafVI plugin is the measurement of pixel intensity of individual objects (leaves) in the Red, Green, and Blue channels and the calculation of various colorimetric visual indexes (CVIs) from these data (figure 1C). The RedGreenBlue measurement can be run on all images saved in a single folder at once (we analyzed up to 446 images at a time), and the results are saved as a .csv file in the same folder. Images that can be used as input are preferably white-balanced and segmented, but the measurements can be run on unprocessed images as well, although this may result in poor identification of individual objects.

To measure the R, G, and B pixel intensities of individual objects in an image, a mask is made that selects individual objects in a similar manner as

in the segmentation step. It then splits the original image into Red, Green, and Blue channels and overlays the mask on each of the channels. The minimum, maximum, median, and mean pixel intensity of each object of the mask is then measured for each of the channels, and written to the results file. The mean values of the Red, Green, and Blue channels are used to calculate the different visual indexes that are used to estimate Chl content: Green:Red ratio (GR_ratio), Red:Green ratio (RG_ratio), Kawashima index (Kawashima), Green Leaf Index (GLI), Normalized Difference Index (NDI), normalized Red (Red_norm), normalized Green (Green_norm), normalized Blue (Blue_norm), and the Woebbecke index (Woebbecke). The results file also contains a column with the image name, the region of interest (ROI), which refers to individual objects in the image, their area, and an x- and y- coordinate that can be used to retrace to which object a measurement refers.

Since ImageJ scans for objects in a left-to-right and top-to-bottom order, the top left object will be the first to be detected and the bottom-right the last. This can be taken into account when preparing multiple leaves in one image, for example by making sure that the objects are ordered top-to-bottom or by arranging the objects in a diagonal from left to right (figure 1). Alternatively, each leaf or plant can be imaged individually. For high-throughput purposes, we advise creating a metadata file that links the image name to the content of the image, which can then be merged with the results file for further analysis.